Research article

Effect of Some Parameters on Optical Soliton Pulses in Photonic Crystal Fibers

Mohammed Salim Jasim

¹Gifted Guardianship Committee, Misan, Iraq

Abstract

Fiber optics have been greatly enhanced by photonic crystal fibers based on microstructured air-glass designs. On the one hand, such fibers enable very tight light confines in a small mode shape region, resulting in significantly improved alternative options between light and dielectric medium. Photonic crystal fibers, on the other hand, allow light to be guided via air core instead of glass. As a result, the latter form of fiber decreases optical nonlinearities in ways that classic fiber designs cannot. The chirp effect and dispersion of photonic crystal fibers with super-Gaussian pulses during various pulses durations are examined in this paper in both normal and anomalous dispersion patterns. The chirp effect and fiber dispersive nonlinear effects are investigated. For this study, a mathematical model of the solution of a nonlinear equation involved the split-step Fourier method. Peak power was reduced for broad pulses. When the magnitude of the super-Gaussian pulse increased proportionally, pulse constriction was also noticeable, Furthermore, the results reveal that an anomalous dispersion system was superior to a regular dispersion system for pulse . The experimental findings will facilitate further research into more understanding of photonic crystal fibers, and to improve data speeds in modern optical communication systems.

1. Introduction

Photonic crystal fibers (PCFs) are very important in modern systems due to their superior properties to traditional fibers. Due to their considerable flexibility in design and high nonlinearity, PCFs outperform traditional optical fibers [1]. A PCF is an optical fiber having a low regular index material in the background and a high index material in the foreground [2]. Light can be guided within a PCF by changing total internal reflection or photonic band-gap guiding by adjusting birefringence, chromatic dispersion, and other optical characteristics [3]. In order to determine

---

*Corresponding author: E-mail: msjadr72@gmail.com

non-linearity, loss of confinement, and effective mode area, photonic crystal fiber is used. PCFs have exceptional qualities and capabilities due to their unique geometric structure, which makes them ideal for sensing applications. PCFs are often designed to provide zero dispersion wavelengths (ZDW) at the desired wavelength. As a result, PCFs are a better choice than traditional optical fibers for a variety of applications including supercontinuum generation, biomedical imaging, meteorology, industrial equipment, and many others [4]. Figure 1 shows a PCF.
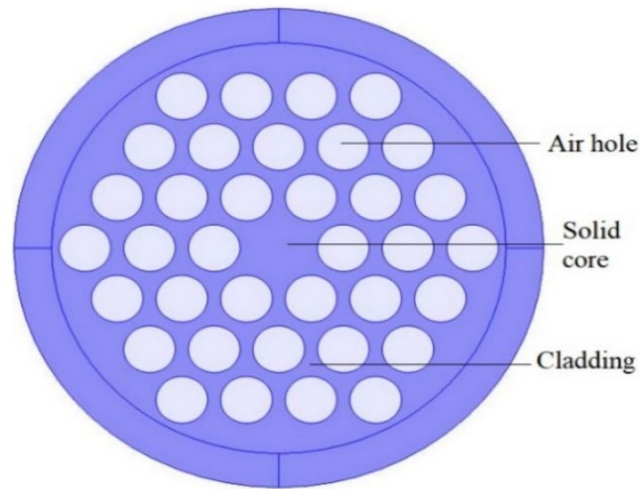

Figure 1. Solid core PCF with microstructure cladding is the most prevalent design [4].

An option for expanding capacity of a PCF is to reduce the canal, and yet another competing option is to increase the transmission speed. As a result, it is beneficial to concentrate on employing laser sources that generate ultra-short pulses, which might result in a variety of nonlinear effects that must be studied. When various wavelengths have different refractive indices, group velocity dispersion (GVD) arises. The data rate is limited by pulse broadening. The GVD effect is integrated into the photonic crystal fiber through a variable represented by β_2. Because the refractive index is affected by the intensity, it creates nonlinearity and induces nonlinear chirp in the pulse [5, 6]. The main nonlinear effect is self-phase modulation [7]. When GVD and chirp are combined, the outcome is a pulse response that is radically distinct from nonlinear effects; the action is also determined by dispersion regions such as the normal (NDR) and abnormal (ADR) regions of dispersion. The value of β_2 for an abnormal dispersion region (ADR) will be less than zero, whereas the value of β_2 in a normal dispersion region (NDR) is larger than zero. Super-Gaussian pulses and their distinct transmission qualities in both the dispersive and chirp effects regions for various pulses durations and super-elevation properties were investigated. These pulses tend to expand much more than Gaussian pulses because their leader and tailed edges are sharper [8]. The shape of super-Gaussian pulses is comparable to that of a square digital pulse, and the shape is one benefit of using them. To study of super-Gaussian pulse dispersion and chirp effects, the nonlinear Schrodinger equation (NLSE) was used to examine PCF phenomena of two types of GVD, and chirp. Because of the complicated nature of the super-Gaussian pulse, this equation was not analytically solvable. As a result, numerical approaches were employed [9]. The Fourier split-step method is the most often used well-known numerical technique for solving it [10]. The answer is computed in many tiny stages throughout the length of the optical cable with this approach [11].

2. Materials and Methods

The Gaussian distribution may be used to estimate the majority of laser pulses. The input field for super-Gaussian pulse has the form shown below [6].

$$U(0,t) = \exp\left[-\frac{1}{2}\left(\frac{t}{T_o}\right)^{2m}\right] \tag{1}$$

Here (t) is a time reference that moves with the GVD, T_o symbolizes half the pulse width, while (m) is the factor that defines the sharpness of the pulse peaks. Because raising (m) causes the spectrum of a pulse to widen, the pulse becomes more broadened as the value of m rises.

NLSE, which is developed using numerical approaches, is used to explore the features of super-Gaussian pulses in the context of GVD alone or in connection with other phenomena such as nonlinear effect. The mathematical representation of NLSE is given as follows:

$$i\frac{\partial U}{\partial z} + \frac{i\alpha}{2}U - \frac{\beta_2}{2}\frac{\partial^2 U}{\partial t^2} + \gamma \,|U|^2 U = 0 \tag{2}$$

Equation (2) illustrates the transmission of an incident electromagnetic wave under the effects of dispersion (β_2), loss(α), and nonlinearity(γ). The variables U and z denote the amplitude pulse and the fiber distance traveled, respectively. By setting loss(α) and nonlinearity(γ) to zero, the impact of GVD on a light signal is investigated using the split-step Fourier method (SSFM), which is one of the better numerical methods for applying in NLSE [12]. Equation (1) is a better choice in the following format for implementation:

$$\frac{\partial U}{\partial z} = (\hat{D} + \hat{N}) \tag{3}$$

$\hat{D}$ is a function that represents fibre dispersion and loss in the assumptions of a linear media, and $\hat{N}$ adjusts for the nonlinear effects of the fiber.

$$\hat{D} = -\frac{\alpha}{2} - \frac{\beta_2}{2}\frac{\partial^2}{\partial t^2} \tag{4}$$

$$\hat{N} = i\gamma \,|U|^2 \tag{5}$$

The SSFM can solve NLSE numerically by supposing that pulse transmission occurs in extremely short steps with value h. There are two phases to this operation, in stage one, only dispersion is active, and N value is zero; while, in stage two, D is deactivated, and only a nonlinear effect is active in the fiber [13]. The PCF material is made up of a number of sections , and each section is of length - h. Upon transmission in a certain part h, dispersion operates initially for a distance of $h/2$, and the nonlinear effect is applied to the entire section at the midway planes. Then, the electromagnetic field is subsequently propagated over the remaining distance of h/2. This completes the pulse transmission in section h, and the procedure is repeated along the entire length of the photonic crystal fiber, concluding with the resolution of the NLSE [14].

3. Results and Discussion

A PCF of the type discussed was considered, with a wavelength of 1.55 μm. The values of $\alpha = 0.02\ dB/km$, $\beta_2 = 0.15\ ps2/km$, chirp C= 0, while the nonlinear coefficient was $\gamma = 0.5\ W^{-1}Km^{-1}$. For different values of T_0, such as (2.5, 3.5, and 4.5) ps, the super-Gaussian pulse was transmitted. It is preferable to optimize data rate by lowering T_0 in optical fiber systems. The effect of reducing T_0 is demonstrated in this research.

3.1 The effect of various m values on the super-Gaussian pulse

Tor begin with, we use a super-Gaussian pulse with a width of T_0 = 4.5 ps. Using equation 1, the shapes of the pulse for different values of m are displayed in Figure 2. The pulse edges become wider as m increases. As a result, as the quantity of m grows larger, the dispersion of super-Gaussian pulses expands as well.
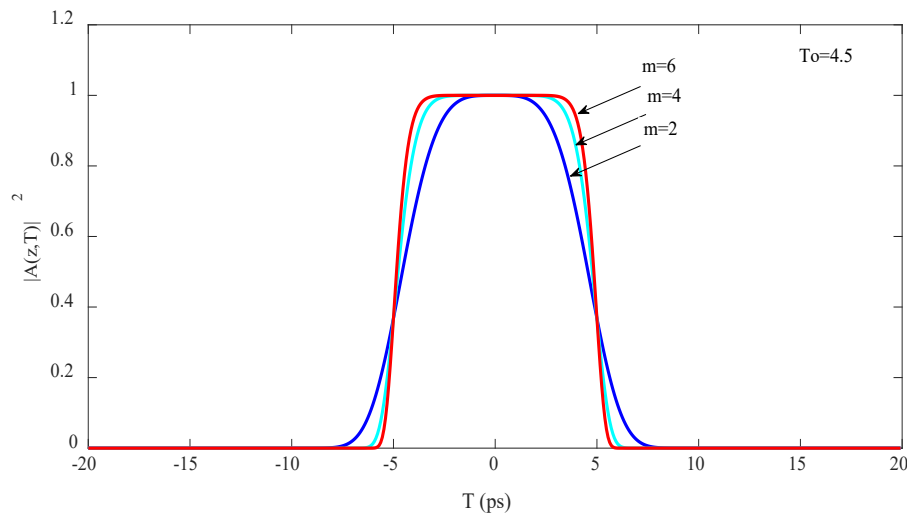

Figure 2. The effect of various m values on the super-Gaussian pulse

3.2 Peak intensity fluctuation along the the fiber for m = 2,4,6

With a variation of T_0, the evolution characteristics of the super-Gaussian pulses shifts. T_0 is reduced to 3.5ps and 2.5 ps in terms of enhancing transmission of data, and the pulse's evolution behavior is investigated for a range of m values. For m = 2, Figure 3 depicts the propagation of a super-Gaussian pulse. Figure 3 also indicates that when the value of T_0 lowers, the peak amplitude reduces. For lowest values of t_0, this means that the optic disperses the pulse more dramatically. Only pulse widening is shown in Figure 2, but greater values of m result in pulse constriction, as illustrated in Figures 4 and 5. In Figure 4, with T_0 = 3.5 ps and 4.5 ps, the super-Gaussian pulse begins to be compressed in the first path length before broadening. The distance to which the pulse compresses reduce as the value of T_0 reduces, with the worst case occurring at T_0 = 2.5 ps.
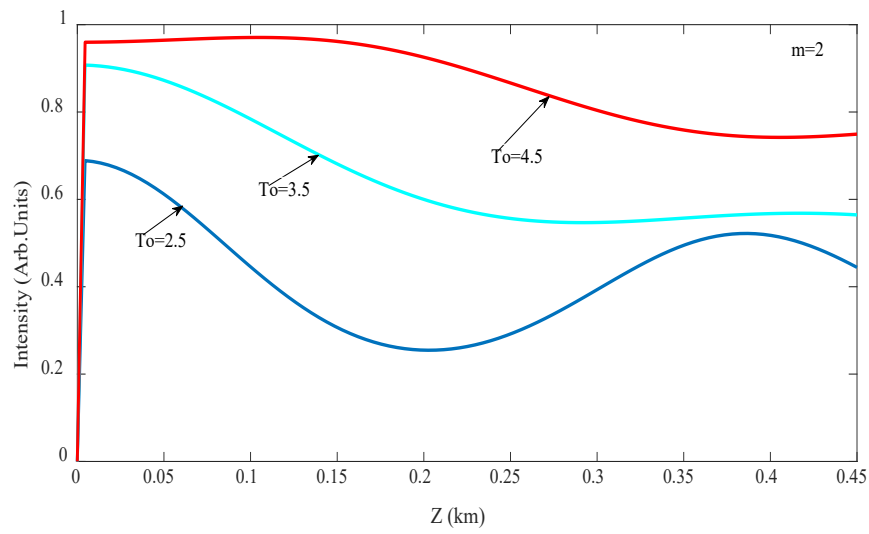
Figure 3. Peak intensity fluctuation along the length of the fiber for m = 2
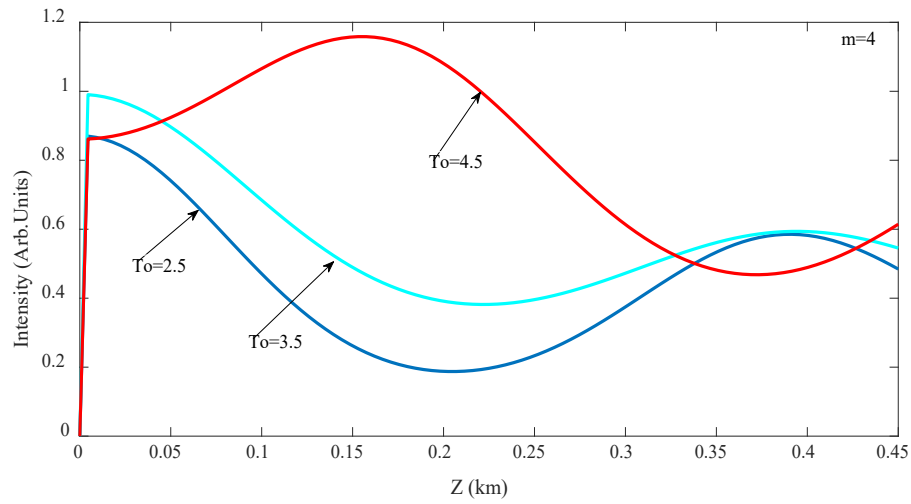

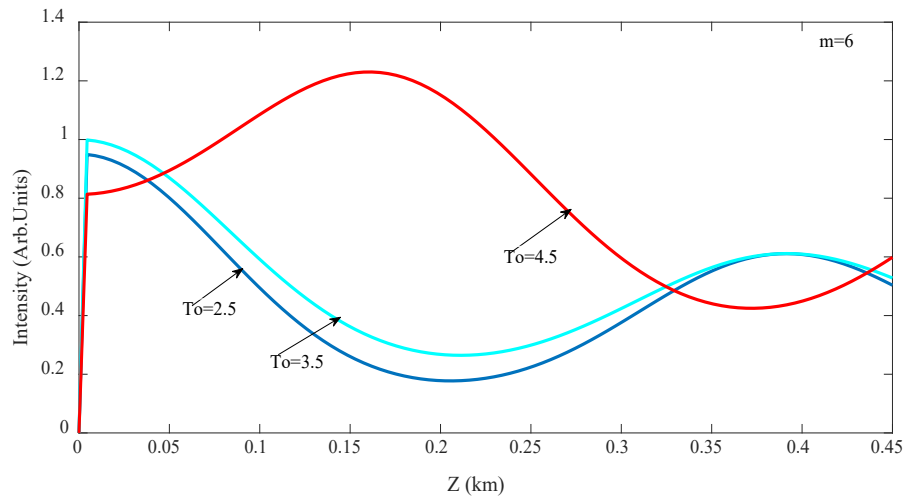**Figure 4.** Peak intensity fluctuation along the length of the fiber for m = 4

Figure 5. Peak intensity fluctuation along the length of the fiber for m = 6

At T_0 = 4.5 ps, remarkable behavior is exhibited, with only compression observable in this scenario for the duration under investigation. However, the consequence of choosing T_0 = 4.5 ps is that the output rate is lower than when using T_0 = 3.5 ps or 2.5 ps. When comparing Figure 4 and Figure 5, it can be seen that the amplitude of the maximum output grows as the value of adjustment increases. Although the amplitude of peak power rises in Figure 5, further study reveals more broadening of the pulse at m = 6 than at m = 4. Where at m = 6, the sharper edges result in the same distance. Peak output intensity versus distance is displayed in Figure 6 for m = 2, 4, and 6 for a stable value of T_0 of 3.5 ps.
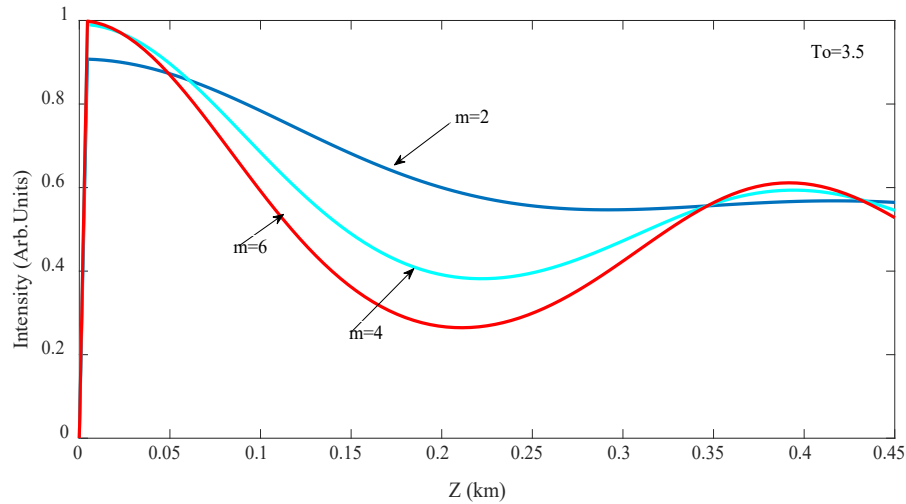

Figure 6. Peak output intensity against distance (z) for
m = 2, 4, 6, and t_0 = 3.5 ps

The induction of dispersion widening of the super-Gaussian pulse at long distances rises when the value of m is raised, as seen in Figure 6. This occurs because as the value of m increases, the super-Gaussian pulse edges get sharper, and as a consequence, the pulse spectrum widens, resulting in additional spreading of the pulse. Only the dispersion dominating mode is relevant for the topic above. Fiber effects, involving nonlinearity, occur together in the practical scenario, and the pulse pattern is substantially different when all three effects are present at the same time, as detailed below. Furthermore, various outcomes are seen depending on the procedure region, in other words, normal versus abnormal dispersion regimes.

3.3 Comparison between ADR GVD and NDR GVD at T_0 = 2.5 ps

For T_0 = 2.5 ps and P = 35 mw, Figure 7 shows the propagation of a single super-Gaussian pulse in a normal dispersion region (NDR) in comparison to an anomalous dispersion region (ADR) in the presence of loss across a 0.25 km length. However, in ADR, the two chirps caused by GVD and nonlinearity have different signs, thus they contend with each other, resulting in less widening than GVD alone in NDR. This reveals an important and significant phenomenon: ADR is a superior region for pulse restoration than NDR. Figure 7 illustrates the identical example with T_0= 3.5 ps. The similar actions of the super-Gaussian pulse is seen. Looking at Figures 7 and 8, it is clear that extending the pulse width raises the maximum output of the pulse. Likewise, the pulse widening in ADR is smaller than that in NDR.
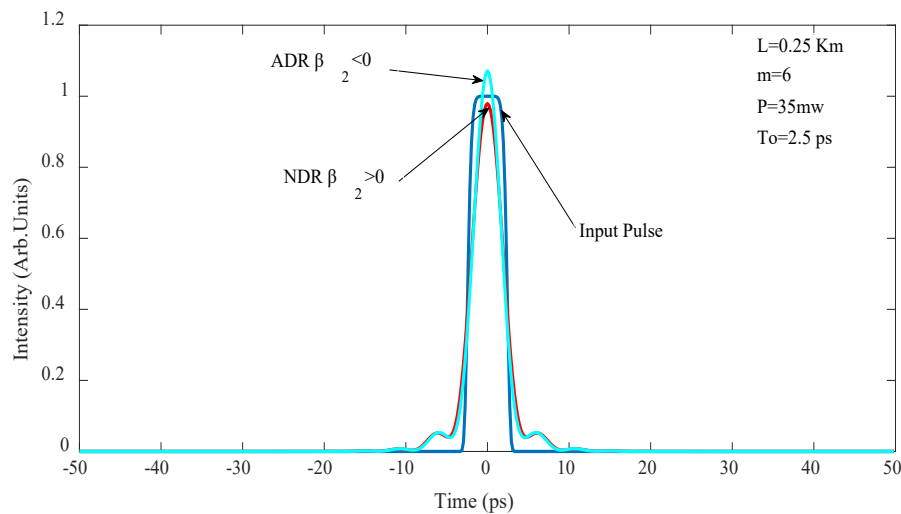

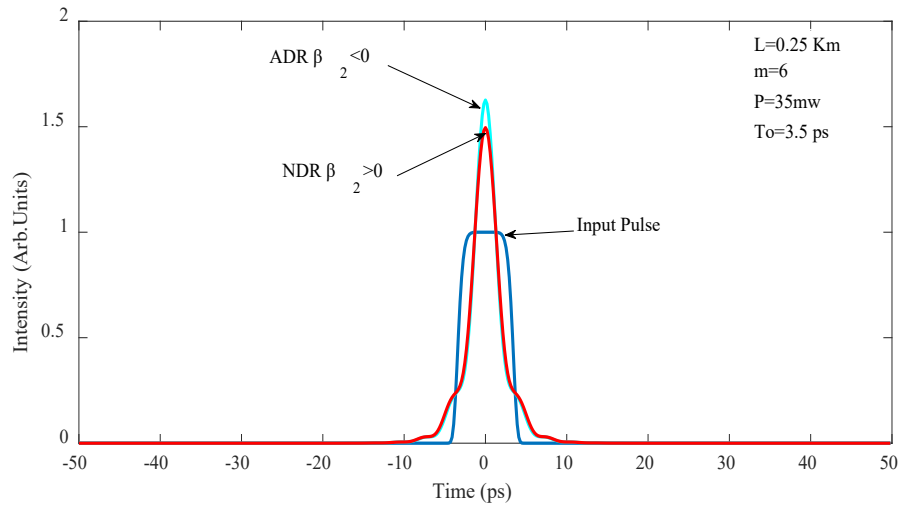**Figure 7.** A comparison between ADR GVD and NDR GVD at T_0 = 2.5 ps

Figure 8. A comparison between ADR GVD and NDR GVD at $T_0 = 3.5$ ps

3.4 Comparison super-Gaussian pulse with different values of chirp

A super-Gaussian pulse was studied according to the equation below [15, 16].

$$U(0,t) = \exp\left[-\frac{1 + iC}{2}\left(\frac{t}{T_0}\right)^{2m}\right] \qquad (6)$$
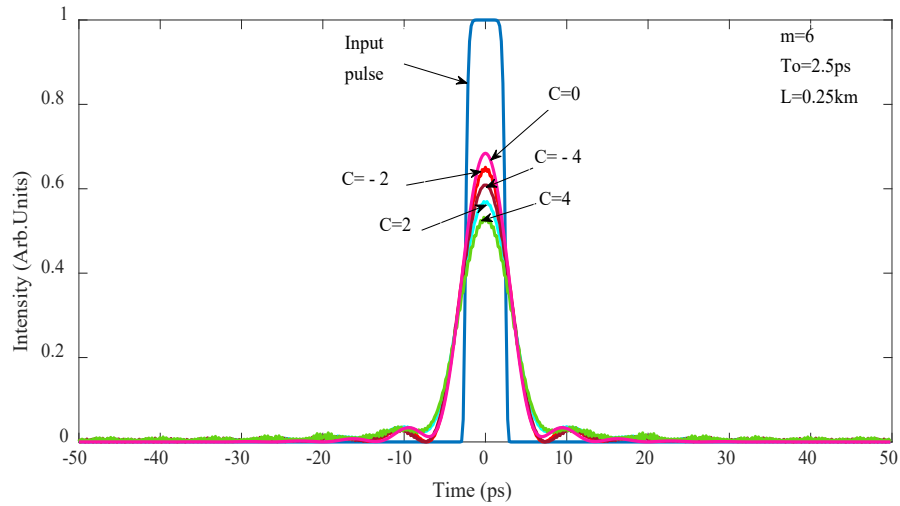
Where C=0,-2,2,-4,4, Figure 9 is obtained.

Figure 9. Illustration of a super-Gaussian pulse at the beginning and end of the photonic crystal fiber

The high amplitude of the pulse in the case of $C = 0$ is obvious, and by dispersion effect, the conservation of energy causes a reduction in pulse amplitude. The widening impact generated by the GVD is increased as the amplitude of the chirp changes in the situations $C = = \pm 2$, ± 4 and the amplitude decreases.

4. Conclusions

The findings of the investigation of the degrading effects of photonic crystal fiber on super-Gaussian pulses under impact of dispersion for various pulse width values have been provided. Normal and anomalous dispersion modes were both considered. The SSF approach was used to solve the NLSE for such pulses traveling through photonic crystal fibers. The results show that NDR favors widening, and thus the pulse broadens more than GVD, but in ADR of GVD, the pulse broadening is reduced. When compared to GVD alone, the maximum output of the pulse rises. These results clearly indicate that ADR is superior to NDR in a single mode optical fiber for pulse restoration, and the features of the regime in which the pulse is transmitted. Theoretically, anticipated pulse broadening and chirp effect were confirmed by the numerical analysis of the super-Gaussian pulse moving in the linear regime. It was also demonstrated that pulse widening causes a decrease in pulse amplitude owing to energy conservation. These findings clearly suggest that ADR is superior to NDR for pulse recovery in photonic crystal fibers. This work depicts the growth patterns of super-Gaussian optical pulse transmission in ADR and NDR for a standard single-mode optic, as well as the different values of chirp in super-Gaussian pulse.

References

[1]   Wang, B.T. and Wang, Q., 2018. Sensitivity-enhanced optical fiber biosensor based on coupling effect between SPR and LSPR. *IEEE Sensors Journal*, 18(20), 8303-8310.

[2]   Algorri, J.F., Zografopoulos, D.C., Tapetado, A., Poudereux, D. and Sánchez-Pena, J.M., 2018. Infiltrated photonic crystal fibers for sensing applications. *Sensors*, 18(12), DOI: 10.3390/s18124263.

[3]   Zang, W., Yuan, Q., Chen, R., Li, L., Li, T., Zou, X. and Zhu, S., 2020. Chromatic dispersion manipulation based on metalenses. *Advanced Materials*, 32(27), DOI: 10.1002/adma.201904935.

[4]   Yang, J., Ghimire, I., Wu, P.C., Gurung, S., Arndt, C., Tsai, D.P. and Lee, H.W.H., 2019. Photonic crystal fiber metalens. *Nanophotonics Journal*, 8(3), 443-449.

[5]   Rifat, A.A., Ahmed, R., Yetisen, A.K., Butt, H., Sabouri, A., Mahdiraji, G.A. and Adikan, F.M., 2017. Photonic crystal fiber based plasmonic sensors. *Sensors and Actuators B: Chemical*, 2(43), 311-325.

[6]   Senior, J.M. and Jamro, M.Y., 2009. *Optical Fiber Communications: Principles and Practice*. 3rd ed. London: Pearson Education.

[7]   Agrawal, G., 2013. Optics and Photonics. 5th eds. *Nonlinear Fiber Optics*, Academic Press.

[8]   Murakawa, T. and Konishi, T., 2015. Pulse-by-pulse near 800-nm band power stabilization using all-optical limiter based on self-phase modulation. *Optics Communications*, 344, 134-138.

[9]   Teucher, M. and Bordignon, E., 2018. Improved signal fidelity in 4-pulse DEER with Gaussian pulses. *Journal of Magnetic Resonance*, 296, 103-111.

[10]   Ayela, A.M., Edah, G., Elloh, C., Biswas, A., Ekici, M., Alzahrani, A.K. and Belic, M.R., 2021. Chirped super–Gaussian and super–sech pulse perturbation of nonlinear Schrödinger's equation with quadratic–cubic nonlinearity by variational principle. *Physics Letters A*, 396, DOI: 10.1016/j.physleta.2021.127231.

[11] Kalantari, M., Karimkhani, A. and Saghaei, H., 2018. Ultra-wide mid-IR supercontinuum generation in As2S3 photonic crystal fiber by rods filling technique. *Optik*, 158, 142-151.
[12] Shao, J., Liang, X. and Kumar, S., 2014. Comparison of split-step Fourier schemes for simulating fiber optic communication systems. *IEEE Photonics Journal*, 6(4), 1-15.
[13] Gaiarin, S., Da Ros, F., Jones, R.T. and Zibar, D., 2020. End-to-end optimization of coherent optical communications over the split-step Fourier method guided by the nonlinear Fourier transform theory. *Journal of Lightwave Technology*, 39(2), 418-428.
[14] Deiterding, R., Glowinski, R., Oliver, H. and Poole, S., 2013. A reliable split-step Fourier method for the propagation equation of ultra-fast pulses in single-mode optical fibers. *Journal of Lightwave Technology*, 31(12), 2008-2017.
[15] Chowdury, A., Krolikowski, W. and Akhmediev, N., 2017. Breather solutions of a fourth-order nonlinear Schrödinger equation in the degenerate, soliton, and rogue wave limits. *Physical Review E*, 96(4), DOI: 10.1103/PhysRevE.96.042209.
[16] Anderson, D. and Lisak, M. 1986. Propagation characteristics of frequency-chirped super-Gaussian optical pulses. *Optics Letters*, 11(9), 569-571.